

## Article

# The Development of High-Performance Platinum-Ruthenium Catalysts for the Methanol Oxidation Reaction: Gram-Scale Synthesis, Composition, Morphology, and Functional Characteristics

Vladislav Menshikov <sup>1,\*</sup>, Kirill Paperzh <sup>1</sup>, Yulia Bayan <sup>1</sup>, Yegor Beskopylny <sup>1</sup>, Aleksey Nikulin <sup>1</sup>, Ilya Pankov <sup>2</sup> and Sergey Belenov <sup>1,3</sup>

<sup>1</sup> Faculty of Chemistry, Southern Federal University, Str. Zorge 7, 344090 Rostov-on-Don, Russia

<sup>2</sup> Research Institute of Physical Organic Chemistry, Southern Federal University, 194/2 Stachki Str., 344090 Rostov-on-Don, Russia

<sup>3</sup> Prometheus R&D LLC, 4g/36 Zhmaylova Str., 344091 Rostov-on-Don, Russia

\* Correspondence: vmenshikov@sfedu.ru

**Abstract:** To obtain the PtRu/C electrocatalysts, the surfactant-free (wet) synthesis methods have been used. The structural-morphological characteristics and electrochemical behavior of the catalysts have been studied. The possibility of ranging the crystallite size from 1.2 to 4.5 nm using different reducing agents (ethylene glycol, ethanol, and isopropanol) has been shown. The effect of both the particles' size and the mass fraction of the metal component on the electrochemical surface area (ESA), activity in the methanol electrooxidation reaction (MOR), and tolerance to its intermediate products has been studied. The simple and scalable surfactant-free synthesis method of the highly active PtRu/C electrocatalysts with a different mass fraction of metals, with their tolerance to intermediate products of the oxidation being 2.3 times higher than the commercial analogue, has been first proposed. The authors have succeeded in obtaining the PtRu/C catalysts with the nanoparticles' size of less than 2 nm, characterized by the ultranarrow size and uniform spatial distributions over the support surface, thus having the ESA of more than  $90 \text{ m}^2 \text{ g}_{\text{PtRu}}^{-1}$ .

**Keywords:** nanoparticles; surfactant-free synthesis; methanol electrooxidation; bimetallic nanoparticles; gram-scale synthesis



**Citation:** Menshikov, V.; Paperzh, K.; Bayan, Y.; Beskopylny, Y.; Nikulin, A.; Pankov, I.; Belenov, S. The Development of High-Performance Platinum-Ruthenium Catalysts for the Methanol Oxidation Reaction: Gram-Scale Synthesis, Composition, Morphology, and Functional Characteristics. *Catalysts* **2022**, *12*, 1257. <https://doi.org/10.3390/catal12101257>

Academic Editor: Carlo Santoro

Received: 29 September 2022

Accepted: 13 October 2022

Published: 17 October 2022

**Publisher's Note:** MDPI stays neutral with regard to jurisdictional claims in published maps and institutional affiliations.

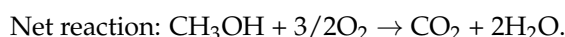
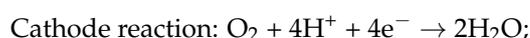
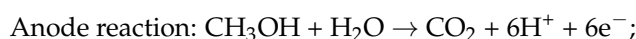


**Copyright:** © 2022 by the authors. Licensee MDPI, Basel, Switzerland. This article is an open access article distributed under the terms and conditions of the Creative Commons Attribution (CC BY) license (<https://creativecommons.org/licenses/by/4.0/>).

## 1. Introduction

The fuel cells based on the direct electrooxidation of alcohols (direct alcohol fuel cells, DAFC) are promising electrical power sources for the devices used in areas with difficult access, including ones with lower temperatures [1]. Alcohols as energy carriers are relatively easy to store and transport, normally having high energy densities [2]. Moreover, DAFC can be attractive due to the simplicity of design, with the latter being critical to develop an effective power source for portable devices [1,2].

The simplest and best-studied type of DAFC is direct methanol fuel cells (DMFC), in which the following reactions proceed [2]:



For these cell reactions to proceed, the cathodic and anodic areas are to obtain a Pt-based electrocatalyst ensuring the high-performance course of the processes [1]. The

reaction pattern of the methanol and other alcohols oxidation on platinum was first proposed by Bagotzky [3] and then by Watanabe and Motoo [4]. Intermediate products, such as formic acid, formaldehyde, carbon monoxide, are known to appear in the system during the anode reaction [5]. The CO molecules are well-known catalytic poisons, with the former being chemisorbed on the surface of the Pt-based nanoparticles (NPs) and decreasing the material's catalytic characteristics, thus leading to its degradation [4,6]. To increase the durability of a catalyst and a resulting device, one needs the additional oxidation of intermediate products up to CO<sub>2</sub> [2].

The platinum-ruthenium catalyst is thought to be the most effective material for the electrooxidation of methanol [3,7–9]. Many researchers [3,7] assume that the reaction of the methanol oxidation on the PtRu surface of NPs might proceed via the bifunctional mechanism, with chemisorption and dehydrogenation of the methanol molecule occurring on the Pt atom, while oxidation of the chemisorbed CO particles occurs with the participation of the OH-groups adsorbed mostly on the surface of ruthenium [3,10]. Gasteiger [11] and Abruna [12] point out that ruthenium is capable of decreasing the dissociation potential of water, thus resulting in the presence of more OH<sub>ads</sub> to accelerate the CO oxidation, as well as inhibiting the CO adsorption due to the change in the electronic structure of Pt (a ligand effect) [8,13].

The materials' structural-morphological parameters caused by the selected synthesis method of particles are known to affect the electrochemical characteristics of the electrocatalysts based on PtRu NPs [14,15]. There are several major factors affecting the PtRu/C catalysts' activity, such as the alloy composition [16–19], the distribution uniformity, the morphology [20], the shape and size of particles [8,21,22], which depend on the preparation technique, and the electronic state [23].

To obtain PtRu NPs on the surface of the carbon support, various methods are applied, among which there are the reduction in the aqueous medium using the sodium borohydride as a reducing agent [24], using the stabilizing agents [14,25], the microwave method [26] at higher temperatures in a stream of hydrogen [27,28], and the sol-gel method based on the ruthenium oxide [29].

The choice of an optimal synthesis method, which could be scaled and used in the production process, as well as allows for the attainment of the catalysts with advanced electrochemical characteristics, is still an urgent task for hydrogen energetics and materials chemistry [15].

This study is aimed at developing and optimizing the existing method to obtain the PtRu/C catalysts characterized by a uniform distribution of NPs over the support surface and their narrow size distribution for platinum and ruthenium to be used in the most effective way. Moreover, it is hypothesized that the proposed method to obtain catalysts could be scaled for further commercial application of the synthesis.

## 2. Results

### 2.1. Structural-Morphological Characteristics of the PtRu/C Catalysts Obtained

A size of the particles formed under conditions of the liquid-phase synthesis is known to be defined in the first turn by a reductant type [22,30], a temperature, a composition [31], and pH of the reaction medium [32–34]. To obtain the PtRu/C materials, the surfactant-free synthesis methods were used, with ethylene glycol, ethanol, and isopropanol being used as reducing agents.

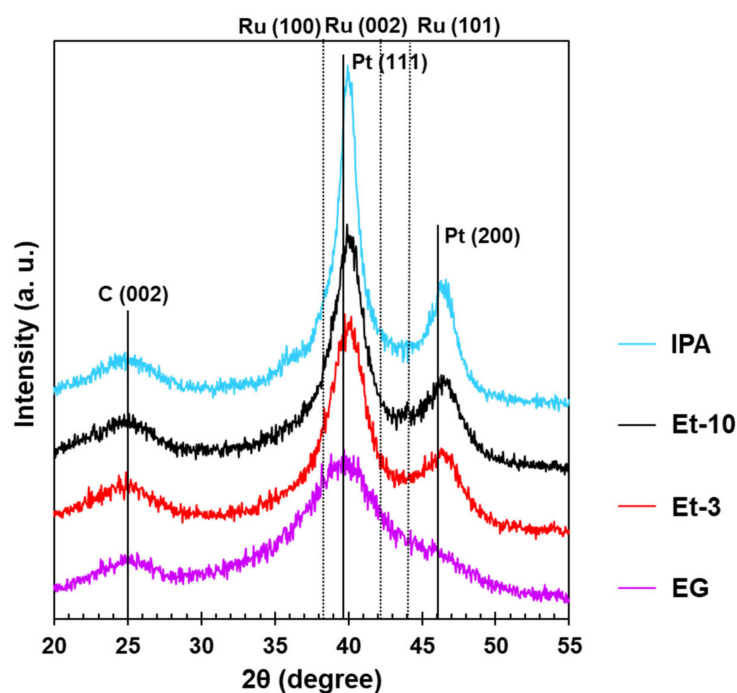
A series of the PtRu/C materials with the metals' mass fraction of about 30% (Table 1) and the Pt loading of 19% were obtained by different synthesis methods. It is noteworthy that during the synthesis using ethanol as a reducing agent, the molar ratio of alkali to platinum-ruthenium was 3 and 10 for Et-3 and Et-10, respectively. The previous works [32–35] show that the bimetallic particles obtained have a smaller size and a narrower size dispersion, with the reaction medium's pH being increased.

**Table 1.** Composition, phase, and structure of the platinum-ruthenium materials.

Sample	Metal Loading, %	Pt Loading, %	Pt:Ru Atomic Ratio	$D_{AV}$ , nm (XRD)	Crystal Lattice Parameter, Å	$D_{NP}$ , nm (TEM)
EG	27.2	19.3	PtRu <sub>0.8</sub>	1.2	3.917	1.9
Et-3	27.4	19.4	PtRu <sub>0.8</sub>	2.6	3.891	2.6
Et-10	27.0	19.0	PtRu <sub>0.8</sub>	3.1	3.884	3.0
IPA	28.0	18.4	PtRu	4.5	3.895	—

The composition of the metal component determined by the X-ray fluorescence analysis (XRF) proved to be PtRu<sub>0.8</sub> for the EG, Et-3, and Et-10 samples and PtRu for the IPA material (Table 1).

The X-ray diffraction patterns for all the Pt-based materials studied demonstrate the characteristic reflections of the carbon support C (002) in the range of values  $2\theta$  of about 25 degrees and the reflections of the metal phase of platinum with the face-centered cubic (FCC) structure (Figure 1). At the same time, the X-ray diffraction patterns have the appearance typical for the platinum-carbon materials containing metal NPs [22,36]. The shift of the most intense reflection peak of platinum (111) to the high-angle region  $2\theta$ , as well as the decrease in the crystal lattice parameter observed for the bimetallic catalysts are connected with the solid solution formation (Figure 1). The latter is due to embedding the ruthenium atoms into the platinum crystal lattice, thus decreasing the interatomic spacing, which is typical for these bimetallic NPs [22,36]. Meanwhile, there are no individual peaks of the phase of ruthenium and its oxides with the typical hexagonal close-packed (HCP) structure in the X-ray diffraction patterns of the catalysts [37]. Nevertheless, there is a possibility of the presence of the materials' amorphous ruthenium oxides, which fail to be revealed by the powder diffraction analysis [37].

**Figure 1.** X-ray diffraction patterns of the PtRu/C materials obtained by the ethylene glycol, ethanol, and isopropanol synthesis methods.

The average crystallite size estimated from the broadening of the most intense peak in the X-ray diffraction patterns using the Scherrer formula grows in the order EG < Et-3 < Et-10 < IPA from 1.2 to 4.5 nm (Table 1).

From the TEM micrographs of the randomly selected surface fragment, the average size of particles in the samples studied was calculated and the histograms of their size distribution were plotted (Figure 2). The average size of NPs estimated by TEM in the EG, Et-3, and Et-10 samples increases from 1.9 to 3.0 nm (Table 1), with the former exceeding the crystallite size, which is normal due to the fact that NPs may consist of several crystallites and the principles of calculating the average size of NPs by XRD and TEM differ to some extent [38–40]. Nevertheless, the values of the average sizes of crystallites and NPs for the materials obtained are close (Table 1). It is worth noting that not only the wide size dispersion of particles, but also the presence of a substantial number of aggregates are typical for the Et-10 sample compared with the Et-3 and EG materials (Figure 2c,d). A similar result of the effect of pH on a size and a distribution of particles over the support surface was obtained by Ohkubo Y. et al. [20]. The increase in pH was conducive to both the increase in the average size of particles and the presence of a considerable number of agglomerates. The change in pH during the synthesis of the PtRu/C catalysts requires more detailed consideration.

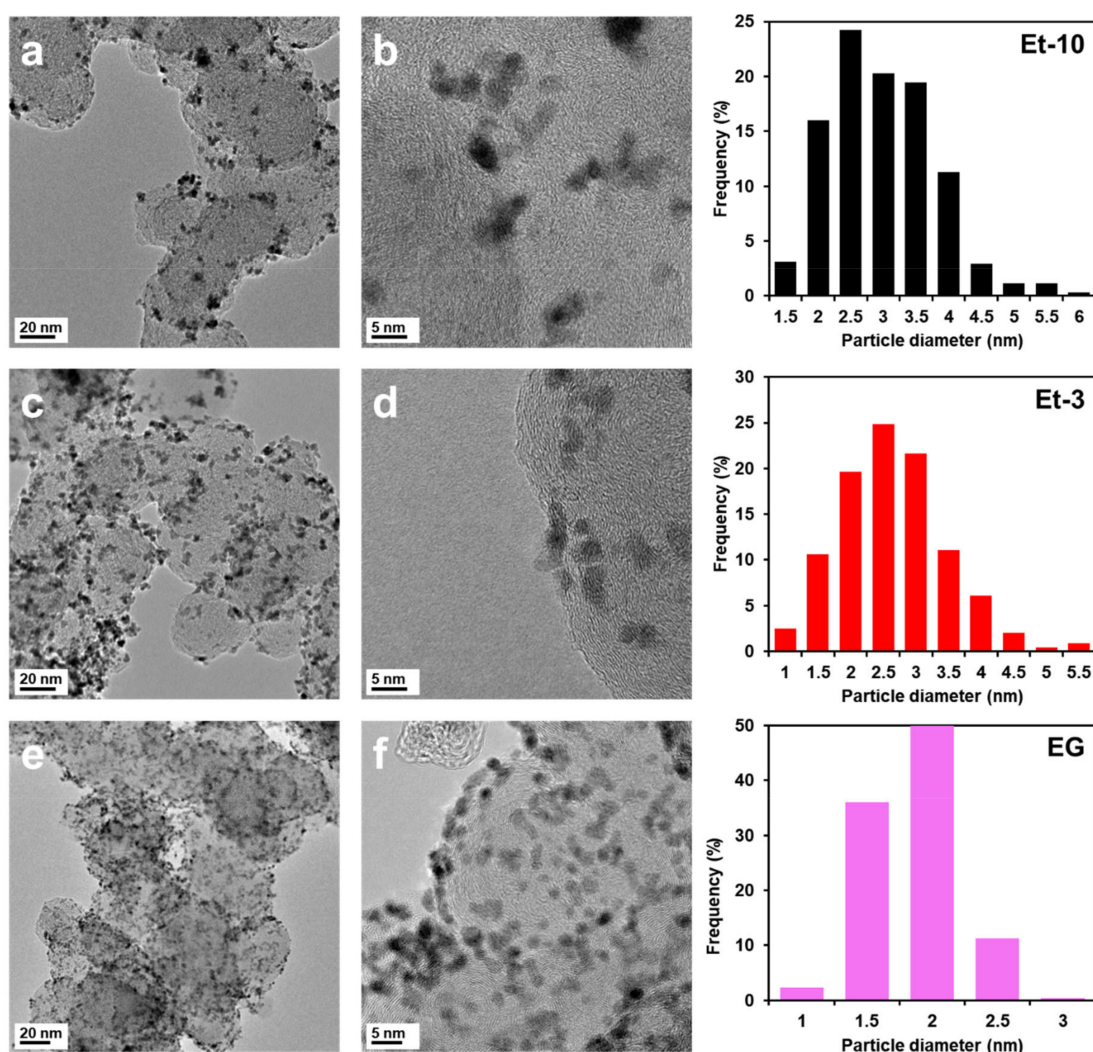


**Figure 2.** TEM micrographs of the Et-10 (a,b), Et-3 (c,d), EG (e,f) samples and histograms of the particles' distribution in the materials.

The most uniform distribution of NPs over the carbon support surface and the narrowest size distribution of NPs are typical for the EG sample (Figure 2e,f).

The results of the elemental mapping of the surface fragment prove the presence of the bimetallic particles in the EG, Et-3, and Et-10 materials (Figures S1–S3).

## 2.2. Electrochemical Characteristics of the PtRu/C Materials

The ESA is a crucial parameter that allows for the estimation of the structural-morphological characteristics of the PtRu/C materials integrally [41,42]. Providing the mass fraction of metals is close, the smaller the particles' size in the material and the more uniform their spatial distribution, the higher the ESA values [36]. The voltammograms presented in Figure 3 and corresponding to the CO oxidation process in the PtRu/C catalysts studied demonstrate the presence of one pronounced peak between 0.4 and 1.0 V (Figure 3). No CO oxidation peak was observed at the second cycle (Figure S2). The ESA values of the PtRu/C materials obtained were estimated from the quantity of electricity spent on the oxidation of the desorbed CO monolayer (see the Experimental Section). The ESA values decrease in the order EG < Et-3 < Et-10 < IPA, which correlates with the increase in the particles' sizes (Tables 1 and 2).

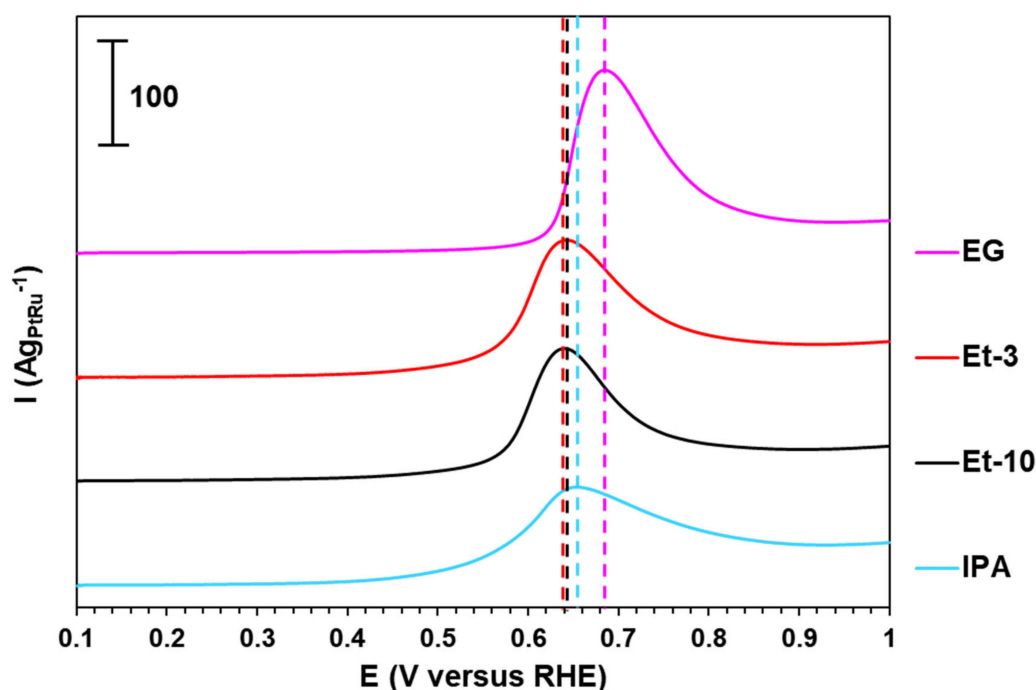


**Figure 3.** Voltammograms of the CO electrochemical desorption for the PtRu/C catalysts. The electrolyte is 0.1 M HClO<sub>4</sub>. The potential sweep rate is 40 mVs<sup>-1</sup>.

**Table 2.** Electrochemical characterizations for the PtRu/C materials by CO-stripping voltammetry.

Sample	E <sub>ONSET</sub> , V	E <sub>PEAK</sub> , V	ESA <sub>CO</sub> , m <sup>2</sup> g <sub>PtRu</sub> <sup>-1</sup>
EG	0.56	0.69	114
Et-3	0.43	0.64	91
Et-10	0.44	0.64	81
IPA	0.41	0.66	70

It is of interest that the onset potential and the peak potential of the CO oxidation for the EG material compared with the other PtRu/C samples are shifted to a more positive region by 130 ± 10 mV and 35 ± 15 mV, respectively (Table 2, Figure 3). This phenomenon can be due to a smaller size of NPs in the EG material [43,44].

Activity of the PtRu/C materials in the MOR was studied by cyclic voltammetry. The CVs for the PtRu/C catalysts demonstrate two characteristic peaks [45] of the direct and reversed courses of the potential sweep, with the direct course of the potential sweep or the typical direction indicating that CV is recorded from the forward sweep (0.05–1.2 V

vs. RHE) to the backward sweep (1.2–0.05 V vs. RHE) (Figure 4a). The peak of the direct course of the potential sweep is known to be due to the methanol molecules' adsorption, followed by their oxidation and the formation of the adsorbed  $\text{HCO}_x$  and  $\text{H}_x$  groups on the platinum surface, with the  $\text{OH}_x^-$  groups being adsorbed on the ruthenium surface [4]. At the same time, it is worth noting that the increase in the potential during CV leads to the accumulation of oxygen groups on the platinum surface and its thorough "blocking" at the potential of the maximum of the direct peak (Figure 4a) [46].

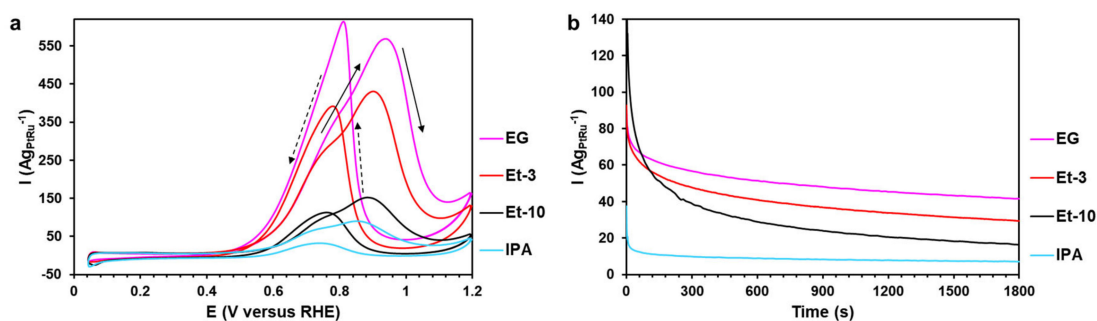


**Figure 4.** (a) Cyclic voltammograms of the PtRu/C materials. The potential sweep rate is  $20 \text{ mVs}^{-1}$ . The electrolyte is  $0.5 \text{ M CH}_3\text{OH} + 0.1 \text{ M HClO}_4$  saturated with Ar under atmospheric pressure. (b) Chronoamperograms at  $0.6 \text{ V}$  for  $1800 \text{ s}$  of the PtRu/C bimetallic alloys in the  $0.5 \text{ M CH}_3\text{OH} + 0.1 \text{ M HClO}_4$  solution.

The  $E_{\text{onset}}$  values of the MOR are close for the EG and Et-3 materials and determined at more negative potentials compared with the Et-10 and IPA samples (Figure 4a, Table 3). The peak current density of the methanol oxidation in the EG sample is 1.3 times higher than the Et-3 material and 3.7 and 6.3 times higher than the Et-10 and IPA materials, respectively. Some authors point out that it is more accurate to compare the specific current density at the potential close to the beginning of the methanol oxidation, generally about  $0.6 \text{ V}$  [47,48].

**Table 3.** Electrochemical characteristics of the platinum-ruthenium materials.

Sample	$E_{\text{onset}}, \text{ V}$	$I_{\text{max}}, \text{ AgPtRu}^{-1}$	$Q_{\text{CH}_3\text{OH}}, \text{ mCgPtRu}^{-1} \times 10^{-5}$	$I_{\text{initial}}, \text{ AgPtRu}^{-1}$	$I_{\text{final}}, \text{ AgPtRu}^{-1}$
EG	0.40	568	64.3	65	42
Et-3	0.40	431	45.0	60	30
Et-10	0.43	152	15.6	62	16
IPA	0.43	90	9.4	12	7

The value of the specific current at  $0.6 \text{ V}$  for the EG and Et-3 materials was  $64 \text{ AgPtRu}^{-1}$ , which was significantly higher than the Et-10 and IPA samples (about  $23 \text{ AgPtRu}^{-1}$ ). To estimate activity in the MOR additionally, the specific quantity of electricity ( $Q_{\text{CH}_3\text{OH}}$ ) spent on the methanol oxidation was calculated by CV of the direct course of the potential sweep [49]. The values of this parameter decrease in the order  $\text{EG} < \text{Et-3} < \text{Et-10} < \text{IPA}$  only as the amount of current at the maximum of the methanol oxidation peaks (Table 3). The results presented testify to the higher electrocatalytic activity in the MOR of the EG and Et-3 samples compared with the Et-10 and IPA catalysts on totality of all the parameters. The enhanced electrocatalytic features of these materials may be due to their structural-morphological characteristics, including a small size of NPs and a composition of PtRu NPs.

Nevertheless, the study [50] notes that the results of the MOR analysis is better to estimate by chronoamperometry rather than by cyclic voltammetry.

According to the results of chronoamperometry at the potential of  $0.6 \text{ V}$  (Figure 4b), the values of the initial ( $I_{\text{initial}}$ ) and final ( $I_{\text{final}}$ ) currents were estimated for all the PtRu/C

catalysts. It should be noted that the materials' catalytic centers are poisoned by intermediate products of the methanol oxidation during the test. With this in mind, it is important to take into account the  $I_{\text{final}}$  values [51,52]. The more the residual value of this parameter, the higher the material's tolerance to intermediate products of the methanol oxidation [52]. In Figure 4b, an abrupt decrease in the currents' values is observed for the first 300 s, which is caused by the adsorption of the methanol oxidation products [51,52]. The current density of the MOR decreases with time since the CO groups and the other intermediate products are easily adsorbed on Pt, thus blocking its surface and inhibiting the catalytic activity. However, the presence of atoms of Ru and its oxide forms on the catalyst's surface accelerates the appearance of  $\text{OH}_{\text{ads}}$ , which largely allows for the facilitation of the further oxidation of CO and the other reaction products [50,52,53]. Therefore, the IPA material is characterized by the lowest value of  $I_{\text{initial}}$ , which is by about  $51 \pm 2 \text{ Ag}_{\text{PtRu}}^{-1}$  less than the EG, Et-3, and Et-10 samples (Table 3). Meanwhile, the EG material is characterized by the highest residual current, which may be due to the smallest size of NPs and the uniformity of their distribution over the support surface compared with the rest of the materials (Table 1, Figure 2e,f).

### 2.3. Scaling the Synthesis Method of the PtRu/C Catalysts

The EG material proved to be the most promising one to be used in DMFC in terms of both activity in the MOR and high tolerance to intermediate products of the methanol oxidation. Therefore, the synthesis method of this sample was scaled to obtain 1 g of the PtRu/C catalyst per one experiment. By this synthesis method, a series of the catalysts with the metals' mass fraction of 30%, 40%, and 60% (the EG-30, EG-40, and EG-60 samples, respectively) and with the ratio of platinum-ruthenium equal to 1:1 were obtained to study the effect of the metals content on electrochemical parameters. It is important to clarify that to avoid the formation of a large number of agglomerates, the Ketjenblack EC-300J carbon support with the surface area of about  $800 \text{ m}^2 \cdot \text{g}^{-1}$  was used to synthesize the EG-60 sample. The commercial analogue PtRu-com (60% PtRu loading, where Pt:Ru is close to 1:1, Alfa Aesar) was used as a reference catalyst.

The mass fraction of metals and the composition of the bimetallic component of the samples obtained are presented in Table S1, whereas the X-ray diffraction patterns of the materials are demonstrated in Figure S5. The ESA of the EG-30 material decreased by 7% compared with the EG analogue obtained without scaling the synthesis (Tables 2 and S2). With the mass fraction of metals growing, the ESA values determined by CO-stripping voltammetry decrease in the order  $\text{EG-30} > \text{EG-40} \geq \text{EG-60} > \text{PtRu-com}$  (Figure S4, Table S2). The decrease in the ESA is caused by the growth in the size of NPs due to the increase in the metal component's concentration in the catalyst [54]. In this regard, the potentials of the beginning and the maximum of the CO oxidation ( $E_{\text{ONSET}}$  and  $E_{\text{PEAK}}$ ) are shifted to the region of more negative potentials, with the PtRu loading being increased (Figure S6, Table S2). This appears to be due to the growth in the particles' size, when increasing the loading of metals.

Activity in the MOR and tolerance to intermediate products of the methanol oxidation were estimated as described earlier. The  $E_{\text{onset}}$  values of the EG-60 material and the commercial PtRu-com are more negative than those of the EG-30 and EG-40 samples, as well as those previously synthesized (Tables 3 and S2, Figures 4a and 5a). The current density at the peak maximum of the direct course of the potential sweep ( $I_{\text{max}}$ ) and the quantity of electricity spent on the methanol oxidation increase in the order  $\text{EG-30} < \text{EG-40} < \text{EG-60} < \text{PtRu-com}$  (Table S2). At the same time, the specific current value at 0.6 V for the EG-60 and PtRu-com materials is about  $93 \text{ Ag}_{\text{PtRu}}^{-1}$ , which is higher compared with the activity of the EG-30 and EG-40 samples (about  $63 \text{ Ag}_{\text{PtRu}}^{-1}$ ).

According to the results of chronoamperometry at the potential of 0.6 V (Figure 5b), the  $I_{\text{final}}$  value for all the gram-scale samples obtained exceeds the commercial PtRu-com by about 2.1–2.3 times (Table S2), despite the  $I_{\text{initial}}$  value being close for all the samples (Figure 5b). Given the error margin of electrochemical measurements, it can be concluded

that the change in the metals' mass fraction pursuant to a close composition of the PtRu component does not affect the tolerance of the materials to intermediate products of methanol oxidation.

This result proves that the optimized synthesis methods might further be scaled successfully.

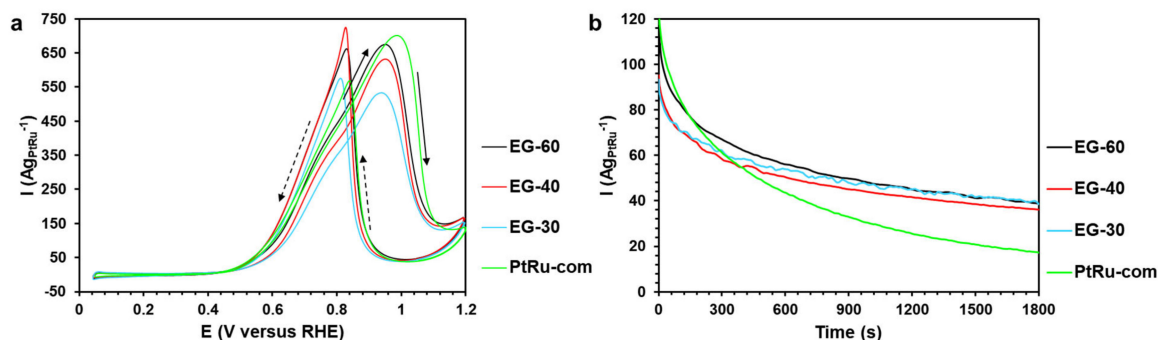


**Figure 5.** (a) Cyclic voltammograms of the PtRu/C materials. The potential sweep rate is 20 mVs<sup>-1</sup>. The electrolyte is 0.5 M CH<sub>3</sub>OH + 0.1 M HClO<sub>4</sub> saturated with Ar under atmospheric pressure. (b) Chronoamperograms at 0.6 V for 1800 s of the PtRu/C bimetallic alloys in the 0.5 M CH<sub>3</sub>OH + 0.1 M HClO<sub>4</sub> solution.

### 3. Materials and Methods

#### 3.1. Chemicals and Materials

In the experimental work, the carbon support Vulcan XC-72 (Cabot Corporation, Boston, MA USA), ethylene glycol (a top grade, not less than 99.8%, Rehacor, LLC, Taganrog, Russia), H<sub>2</sub>PtCl<sub>6</sub>·6H<sub>2</sub>O (TU 2612-034-00205067-2003, mass fraction of Pt 37.6%, Aurat, Moscow, Russia), RuCl<sub>3</sub> (TU 2625-050-00205067-2004, mass fraction of Ru 47.34%, Aurat, Russia), sodium hydroxide (Rehacor, LLC), ethanol (98.0%, JSC Vekton, St Petersburg, Russia), argon (Ar, 99.9%, Globus, Moscow, Russia), isopropanol (99.8%, Ekos-1, Moscow, Russia), and sulfuric acid (JSC Vekton, Russia) have been used.

#### 3.2. The PtRu/C Synthesis with Ethylene Glycol Used as a Reducing Agent

A weighed amount of the carbon support Vulcan XC-72 was homogenized with ultrasound for 2 min at the amplitude of 50% in the beaker containing 100 mL of ethylene glycol. A calculated volume of the 1 M hydrous solution of NaOH was then added with constant stirring to give the molar ratio of alkali to platinum-ruthenium equal to 10. The salts of H<sub>2</sub>PtCl<sub>6</sub>·6H<sub>2</sub>O and RuCl<sub>3</sub> were added in the amount required to obtain the 30% PtRu loading in the samples with the ratio of metals equal to 1:1, and the resulting mixture was heated to 160 °C. After reaching the defined temperature value, the reaction system was allowed to stand for 4 h with constant stirring. The heating was then stopped, and the suspension was allowed to stand at room temperature for 2 h, followed by adding the 1 M solution of H<sub>2</sub>SO<sub>4</sub> to the formed PtRu particles to be completely deposited on the carbon support surface. The product was next filtered and repetitively rinsed with bidistilled water and isopropyl alcohol. The resulting catalyst was desiccator-dried over phosphorus pentoxide for 24 h. The PtRu/C synthesis with ethylene glycol used as a reducing agent is hereinafter referred to as EG.

#### 3.3. The PtRu/C Synthesis with Ethanol Used as a Reducing Agent

A weighed amount of the carbon support Vulcan XC-72 was homogenized with ultrasound for 2 min at the amplitude of 50% in the beaker containing 100 mL of ethanol. A calculated volume of the 1 M hydrous solution of NaOH was then added with constant stirring to give the molar ratio of alkali to platinum-ruthenium equal to 3 or 10. The salts of H<sub>2</sub>PtCl<sub>6</sub>·6H<sub>2</sub>O and RuCl<sub>3</sub> were added in the amount required to obtain the 30% PtRu

loading in the samples with the ratio of metals equal to 1:1, and the resulting mixture was heated to 70 °C. After reaching the defined temperature value, the reaction system was allowed to stand for 4 h with constant stirring. The heating was then stopped, and the suspension was allowed to stand at room temperature for 2 h, followed by adding the 1 M solution of H<sub>2</sub>SO<sub>4</sub> to the formed PtRu particles to be completely deposited on the carbon support surface. The product was next filtered and repetitively rinsed with bidistilled water and isopropyl alcohol. The resulting catalyst was desiccator-dried over phosphorus pentoxide for 24 h. The PtRu/C material obtained at the molar ratio of alkali to platinum-ruthenium equal to 10 is hereinafter referred to as Et-10, the one obtained at the molar ratio of alkali to platinum-ruthenium equal to 3 is hereinafter referred to as Et-3.

#### 3.4. The PtRu/C Synthesis with Isopropyl Alcohol Used as a Reducing Agent

A weighed amount of the carbon support Vulcan XC-72 was homogenized with ultrasound for 2 min at the amplitude of 50% in the beaker containing 100 mL of isopropyl alcohol. A calculated volume of the 1 M hydrous solution of NaOH was then added with constant stirring to give the molar ratio of alkali to platinum-ruthenium equal to 3. The salts of H<sub>2</sub>PtCl<sub>6</sub>·6H<sub>2</sub>O and RuCl<sub>3</sub> were added in the amount required to obtain the 30% PtRu loading in the samples with the ratio of metals equal to 1:1, and the resulting mixture was heated to 70 °C. After reaching the defined temperature value, the reaction system was allowed to stand for 6 h with constant stirring. The heating was then stopped, and the suspension was allowed to stand at room temperature for 2 h, followed by adding the 1 M solution of H<sub>2</sub>SO<sub>4</sub> to the formed PtRu particles to be completely deposited on the carbon support surface. The product was next filtered and repetitively rinsed with bidistilled water and isopropyl alcohol. The resulting catalyst was desiccator-dried over phosphorus pentoxide for 24 h. The PtRu/C materials obtained by the isopropyl alcohol synthesis methods are hereinafter referred to as IPA.

#### 3.5. Thermogravimetry

The mass fraction of platinum ( $\omega$  (PtRu)) in PtRu/C was determined by thermogravimetry related to the (PtRu) mass residue left after burning the PtRu/C (800 °C, 40 min). When calculating the PtRu mass fraction, it was taken into account that the unburned residue left after burning contained Pt and the Ru (IV) oxide. The error margin was  $\pm 3\%$ .

#### 3.6. X-ray Fluorescence Analysis

To determine the ratio of metals in the samples, the method of the X-ray fluorescence analysis on the spectrometer with total external reflection of X-ray radiation RFS-001 (Research Institute of Physics, Southern Federal University, Rostov-on-Don) was used. The sample exposure time was 300 s. Registration and processing of X-ray fluorescence spectra were carried out with the UniveRS software V1.1 (Southern Federal University, Rostov-on-Don, Russia). The obtained X-ray fluorescence spectra were processed with the UniveRS software (Southern Federal University, Rostov-on-Don, Russia), with the resulting accuracy being  $\pm 0.1$ .

#### 3.7. X-ray Examination

The powder diffraction method was used to study structural characteristics of the PtRu/C materials obtained. The ARL X'TRA powder diffractometer with the Bragg-Brentano geometry ( $\theta$ - $\theta$ ), CuK $\alpha$  radiation ( $\lambda = 0.154056$  nm) at room temperature, was used to record the X-ray diffraction patterns. The X-ray diffraction patterns of the samples studied were recorded in the range of angles of  $20 \leq 2\theta \leq 55$  degrees by step-by-step scanning, with the detector movement step being 0.02 degrees [38].

The X-ray diffraction patterns were processed with the SciDavis software V 2.7 to extract the peaks' parameters correctly, this being of particular importance when the peaks overlap over one another in case of small sizes of particles [38]. The calculation of the

average crystallite size ( $D_{Av}$ ) was carried out by the Scherrer formula as described in [55–57].  $D_{Av}$  was calculated using the Scherrer equation as follows:

$$D_{Av} = K\lambda / (\text{FWHM} \cos\theta),$$

where  $\lambda$  is the wavelength of monochromatic radiation (in Å),

FWHM is the full width at half maximum (in radians),

$K = 0.89$  is the Scherrer's constant,

$D_{Av}$  is the average thickness of the "stack" of reflecting planes in the coherent scattering region (in Å),

$\theta$  is the angle of incidence of the X-ray beam (in radians). The error margin was  $\pm 8\%$ .

### 3.8. Transmission Electron Microscopy

The size of PtRu NPs, the features of their size, and spatial distributions were studied by high-resolution transmission electron microscopy (HRTEM). The TEM micrographs were obtained using the JEOL JEM F200 (Tokyo, Japan) and FEI Tecnai G2 F20 S-TWIN (Hillsboro, OR, USA) microscopes with the accelerating voltage of 200 kV, the cold field emission gun with the current of 12–15  $\mu\text{A}$ , the double-tilt Be specimen holder 01361 RSTHB, and the CMOS AMT camera. To prepare the sample for measurements, 0.5 mg of the catalyst were placed in 1 mL of isopropanol and dispersed with ultrasound for 10 min. A drop of the resulting suspension was applied to the standard copper grid covered with a layer of amorphous carbon 5–6 nm thick, thereafter, the sample was dried in air at room temperature for 60 min. The histograms of a platinum NPs' size distribution in the catalysts were plotted, considering that the results of the size determination for at least 400 particles were randomly selected in the TEM micrographs in different regions of the sample. The error margin was  $\pm 0.2$  nm.

### 3.9. Electrochemical Methods of the Study

When obtaining the suspension of the PtRu/C catalysts (the catalytic "inks"), the sample weight was calculated in order that with 8  $\mu\text{L}$  of the catalyst suspension being successively applied to the electrode, the platinum weight should be 20  $\mu\text{g}_{\text{Pt}}\text{cm}^{-2}$ . Then, 100  $\mu\text{L}$  of the Nafion<sup>®</sup> polymer 1% aqueous emulsion were added with the introduction of 1900  $\mu\text{L}$  of isopropyl alcohol (an extra-pure grade). The suspension was dispersed with ultrasound for 25 min at 5–15  $^{\circ}\text{C}$  with alternate stirring every 5 min. The 2  $\mu\text{L}$  aliquot of "inks" was sampled with a pipette tip with constant stirring and applied to the end-face of the polished and degreased glass-carbon disk with the area of 0.196  $\text{cm}^2$ . The electrode was dried in air for 15 min at the rotation of 700 rpm. The 3  $\mu\text{L}$  aliquots of "inks" were similarly applied to the formed catalytic layer for an additional two times.

The electrochemical performance of the catalysts in the standard three-electrode cell was studied by cyclic voltammetry at 23  $^{\circ}\text{C}$  using the potentiostat VersaSTAT 3 (AMETEK, Inc., Berwyn, PA, USA). The silver-chloride electrode was used as a reference, whereas the platinum wire was used as an auxiliary. All the potentials were considered in the work with regard to the reversible hydrogen electrode (RHE). The electrochemical calculations followed exposing the electrode to the electrochemical activation by setting 100 current voltage cycles in the potential range from 0.04 to 1.2 V at the rate of scanning of 200  $\text{mVs}^{-1}$  in the solution of 0.1 M  $\text{HClO}_4$  under the argon atmosphere.

The ESA of the prepared PtRu/C materials was determined by CO-stripping voltammetry. The electrochemical oxidation of CO was studied by purging the deaerated solution of 0.1 M  $\text{HClO}_4$  with the gas for 20 min with the working electrode held at  $E = 0.1$  V. The cell was then purged with Ar for 40 min to remove excess CO. Next, the potential was scanned in the anode direction up to 1.2 V at the sweep rate of 20  $\text{mVs}^{-1}$ . Subsequent recording of two cyclic voltammograms (CVs) in the potential range of 0.04–1.2 V was carried out to check the completeness of the CO desorption from the catalyst surface. The ESA values were calculated in terms of the quantity of electricity spent on the oxidation of the adsorbed CO as described in [58]. The error margin was  $\pm 10\%$ .

The CVs of the MOR were obtained in the 0.1 M HClO<sub>4</sub> solution containing 0.5 M CH<sub>3</sub>OH in the potential range of 0.04–1.20 V (RHE) at the sweep rate of 20 mVs<sup>-1</sup>, when purging the solution with the Ar inert gas. The chronoamperograms were measured at the potential range of 0.6 V for 1800 s, followed by estimating the values of the initial current (*I*<sub>initial</sub>) in 10 s after the beginning of the experiment and the final one (*I*<sub>final</sub>). The error margin was ±10%.

#### 4. Conclusions

With the utilization of simple surfactant-free synthesis methods, the PtRu/C catalysts with a different average size of NPs, but with a close platinum-ruthenium ratio (1:1), as well as with the metals' mass fraction of about 30% have been obtained. Ranging the pH under conditions of the ethanol synthesis method has been shown to affect the morphology and activity of the catalysts significantly. The molar ratio of alkali to platinum-ruthenium equal to 3 has been established to be more optimal than the ratio equal to 10. With the utilization of ethylene glycol as a solvent and a reducing agent during the synthesis of the PtRu/C material, the average size of bimetallic NPs has proved to be smallest, with their spatial distribution being more uniform than the samples obtained with ethanol and isopropanol.

The current density at both the potential of 0.6 V and the peak maximum of the direct course of the potential sweep during the methanol oxidation increases, with the average size of NPs decreasing. Moreover, the EG material is characterized by the highest tolerance to intermediate products of the methanol oxidation.

The possibility of scaling the optimized synthesis methods has been demonstrated when obtaining gram quantities of the PtRu/C catalysts.

The study of the effect of the metals' mass fraction in terms of a close composition of the bimetallic component has been conducted for the scaled synthesis. The increase in the metal component's mass fraction in the PtRu/C materials has been shown to be conducive to the shift of the peak of the methanol oxidation beginning to the region of more negative potentials. The change in the metals' mass fraction does not affect the tolerance of the materials to intermediate products of methanol oxidation.

Therefore, the 56.2% mass of PtRu material EG-60 obtained under conditions of the scaled synthesis is characterized by the similar catalytic activity in the MOR, despite the tolerance to intermediate products of methanol oxidation being 2.3 times higher than the commercial analogue PtRu-com.

This result demonstrates that the samples obtained are promising for use in the membrane electrode assembly (MEA) and the scaled synthesis method presented has high-potential for application in commercial purposes.

**Supplementary Materials:** The following supporting information can be downloaded at: <https://www.mdpi.com/article/10.3390/catal12101257/s1>. Figure S1: The elemental mapping of the surface fragment for the EG sample: The STEM micrograph of the surface (a), the distribution maps of platinum (b), oxygen (c), and ruthenium (d); Figure S2: The elemental mapping of the surface fragment for the Et-3 sample: The STEM micrograph of the surface (a), the distribution maps of platinum (b), oxygen (c), and ruthenium (d); Figure S3: The elemental mapping of the surface fragment for the Et-10 sample: The STEM micrograph of the surface (a), the distribution maps of platinum (b), oxygen (c), and ruthenium (d); Figure S4: CO-stripping, the potential sweep rate is 40 mVs<sup>-1</sup>, the atmosphere of Ar; Figure S5: X-ray diffraction patterns of the PtRu/C materials obtained by the ethylene glycol, ethanol, and isopropanol synthesis methods; Figure S6: CO-stripping, the potential sweep rate is 40 mVs<sup>-1</sup>, the atmosphere of Ar. Table S1: Composition, phase, and structure of the platinum-ruthenium materials; Table S2: Electrochemical characteristics of the platinum-ruthenium materials.

**Author Contributions:** Conceptualization, K.P. and S.B.; methodology, V.M. and S.B.; validation, K.P., S.B. and V.M.; formal analysis, A.N. and Y.B. (Yegor Beskopylny); investigation, K.P. and V.M.; data curation, I.P., Y.B. (Yulia Bayan), Y.B. (Yegor Beskopylny) and V.M.; writing—original draft preparation, K.P. and V.M.; writing—review and editing, V.M. and K.P.; visualization, Y.B. (Yulia

Bayan); supervision, K.P. and S.B.; project administration, S.B. All authors have read and agreed to the published version of the manuscript.

**Funding:** This research was financially supported by the Ministry of Science and Higher Education of the Russian Federation (State Assignment in the Field of Scientific Activity No. 0852-2020-0019).

**Data Availability Statement:** The data presented in this study are available on request from the corresponding author.

**Acknowledgments:** The authors are grateful to Maltsev A.V. for the support in translation and editing processes and the assistance in communication with the editorial board; to Toporkov N.V. for registration and processing of X-ray fluorescence spectra. The authors appreciate the support by LLC “PROMETHEUS R&D” (Rostov-on-Don) and LLC “Systems for Microscopy and Analysis” (Skolkovo, Moscow) for conducting TEM and STEM studies. The authors would like to acknowledge the Southern Federal University Strategic Academic Leadership Program (“Priority 2030”) for the support of graduate students having taken part in this study.

**Conflicts of Interest:** The authors declare no conflict of interest.

## Abbreviations

DMFC	Direct methanol fuel cells
NPs	Nanoparticles
MEA	Membrane electrode assembly
XRD	X-ray diffraction
TEM	Transmission electron microscopy
ESA	Electrometrical surface area
CV	Cyclic voltammetry
MOR	Methanol oxidation reaction
STEM	Scanning transmission electron microscopy
RDE	Rotating disk electrode
RHE	Reversible hydrogen electrode
XRF	X-ray fluorescence analysis

## References

1. Ramli, Z.A.C.; Kamarudin, S.K. Platinum-Based Catalysts on Various Carbon Supports and Conducting Polymers for Direct Methanol Fuel Cell Applications: A Review. *Nanoscale Res. Lett.* **2018**, *13*, 410. [[CrossRef](#)]
2. Wala, M.; Simka, W. Effect of Anode Material on Electrochemical Oxidation of Low Molecular Weight Alcohols—A Review. *Molecules* **2021**, *26*, 2144. [[CrossRef](#)]
3. Bagotzky, V.S.; Vassiljev, Y.B. Adsorption of Organic Substances on Platinum Electrodes. *Electrochim. Acta* **1966**, *11*, 1439–1461. [[CrossRef](#)]
4. Watanabe, M.; Motoo, S. Electrocatalysis by Ad-Atoms: Part II. Enhancement of the Oxidation of Methanol on Platinum by Ruthenium Ad-Atoms. *J. Electroanal. Chem. Interfacial Electrochem.* **1975**, *60*, 267–273. [[CrossRef](#)]
5. Zhao, W.-Y.; Ni, B.; Yuan, Q.; He, P.-L.; Gong, Y.; Gu, L.; Wang, X. Highly Active and Durable Pt<sub>72</sub>Ru<sub>28</sub> Porous Nanoalloy Assembled with Sub-4.0 nm Particles for Methanol Oxidation. *Adv. Energy Mater.* **2017**, *7*, 1601593. [[CrossRef](#)]
6. Tripachev, O.V.; Modestov, A.D.; Korchagin, O.V.; Bogdanovskaya, V.A.; Vasilenko, V.A.; Radina, M.V. Making an Anode of a Hydrogen-Air Fuel Cell More Tolerant to CO: PtRuCo/C Catalyst and Synergistic Effect of PtRu/C and Oxygen Additives. *Russ. J. Appl. Chem.* **2020**, *93*, 1743–1749. [[CrossRef](#)]
7. Da Silva, E.P.; Fragal, V.H.; Silva, R.; Pinto, A.H.; Sequinel, T.; Ferrer, M.; Moreira, M.L.; Camargo, E.R.; Barbosa, A.P.M.; Felipe, C.A.S.; et al. Chapter 28—Nanocatalysts for Fuel Cells. In *Nanotechnology in the Automotive Industry*; Song, H., Nguyen, T.A., Yasin, G., Singh, N.B., Gupta, R.K., Eds.; Elsevier: Amsterdam, The Netherlands, 2022; pp. 579–604.
8. Kuyuldar, E.; Polat, S.S.; Burhan, H.; Mustafaov, S.D.; Iyidogan, A.; Sen, F. Monodisperse Thiourea Functionalized Graphene Oxide-Based PtRu Nanocatalysts for Alcohol Oxidation. *Sci. Rep.* **2020**, *10*, 7811. [[CrossRef](#)]
9. Yuda, A.; Ashok, A.; Kumar, A. A Comprehensive and Critical Review on Recent Progress in Anode Catalyst for Methanol Oxidation Reaction. *Catal. Rev.* **2020**, *64*, 126–228. [[CrossRef](#)]
10. Maiorova, N.A.; Grinberg, V.A.; Pasynskii, A.A.; Shiryayev, A.A.; Vysotskii, V.V. Nanostructured Catalysts of Methanol Electrooxidation Based on Platinum–Ruthenium–Palladium and Platinum–Ruthenium–Iridium Alloys Derived from Coordination Compounds. *Russ. J. Coord. Chem.* **2018**, *44*, 738–744. [[CrossRef](#)]
11. Gasteiger, H.A.; Markovic, N.; Ross, P.N.; Cairns, E.J. Methanol Electrooxidation on Well-Characterized Pt-Ru Alloys. *J. Phys. Chem.* **1993**, *97*, 12020–12029. [[CrossRef](#)]

12. Wang, H.; Alden, L.R.; DiSalvo, F.J.; Abruna, H.D. Methanol Electrooxidation on PtRu Bulk Alloys and Carbon-Supported PtRu Nanoparticle Catalysts: A Quantitative DEMS Study. *Langmuir* **2009**, *25*, 7725–7735. [[CrossRef](#)] [[PubMed](#)]
13. Waszczuk, P.; Wieckowski, A.; Zelenay, P.; Gottesfeld, S.; Coutanceau, C.; Leger, J.M.; Lamy, C. Adsorption of CO Poison on Fuel Cell Nanoparticle Electrodes from Methanol Solutions: A Radioactive Labeling Study. *J. Electroanal. Chem.* **2001**, *511*, 55–64. [[CrossRef](#)]
14. Stoupin, S.; Rivera, H.; Li, Z.; Segre, C.U.; Korzeniewski, C.; Casadonte, J.D., Jr.; Inoue, H.; Smotkin, E.S. Structural Analysis of Sonochemically Prepared PtRu versus Johnson Matthey PtRu in Operating Direct Methanol Fuel Cells. *Phys. Chem. Chem. Phys.* **2008**, *10*, 6430–6437. [[CrossRef](#)] [[PubMed](#)]
15. Ermete, A. Evaluation of the Optimum Composition of Low-Temperature Fuel Cell Electrocatalysts for Methanol Oxidation by Combinatorial Screening. *ACS Comb. Sci.* **2017**, *19*, 47–54.
16. Franceschini, E.A.; Bruno, M.M.; Williams, F.J.; Viva, F.A.; Corti, H.R. High-Activity Mesoporous Pt/Ru Catalysts for Methanol Oxidation. *ACS Appl. Mater. Interfaces* **2013**, *5*, 10437–10444. [[CrossRef](#)]
17. Park, K.-W.; Choi, J.-H.; Ahn, K.-S.; Sung, Y.-E. PtRu Alloy and PtRu-WO<sub>3</sub> Nanocomposite Electrodes for Methanol Electrooxidation Fabricated by a Sputtering Deposition Method. *J. Phys. Chem. B* **2004**, *108*, 5989–5994. [[CrossRef](#)]
18. Jusys, Z.; Kaiser, J.; Behm, R. Composition and Activity of High Surface Area PtRu Catalysts towards Adsorbed CO and Methanol Electrooxidation—: A DEMS Study. *Electrochim. Acta* **2002**, *47*, 3693–3706. [[CrossRef](#)]
19. Tusi, M.M.; Polanco, N.S.D.; Brandalise, M.; Correa, O.V.; Villalba, J.C.; Anaissi, F.J.; Neto, A.O.; Spinace, E. PtRu/Carbon Hybrids With Different Pt:Ru Atomic Ratios Prepared by Hydrothermal Carbonization for Methanol Electro-Oxidation. *Int. J. Electrochem. Sci.* **2011**, *6*, 484–491.
20. Ohkubo, Y.; Kageyama, S.; Seino, S.; Nakagawa, T.; Kugai, J.; Nitani, H.; Ueno, K.; Yamamoto, T. Radiolytic Synthesis of Carbon-Supported PtRu Nanoparticles Using High-Energy Electron Beam: Effect of pH Control on the PtRu Mixing State and the Methanol Oxidation Activity. *J. Nanopart. Res.* **2013**, *15*, 1597. [[CrossRef](#)]
21. Yang, B.; Lu, Q.; Wang, Y.; Zhuang, L.; Lu, J.; Liu, P.; Wang, J.; Wang, R. Simple and Low-Cost Preparation Method for Highly Dispersed PtRu/C Catalysts. *Chem. Mater.* **2003**, *15*, 3552–3557. [[CrossRef](#)]
22. Roth, C.; Martz, N.; Fuess, H. Characterization of Different Pt–Ru Catalysts by X-ray Diffraction and Transmission Electron Microscopy. *Phys. Chem. Chem. Phys.* **2001**, *3*, 315–319. [[CrossRef](#)]
23. Sirk, A.H.C.; Hill, J.M.; Kung, S.K.Y.; Birss, V.I. Effect of Redox State of PtRu Electrocatalysts on Methanol Oxidation Activity. *J. Phys. Chem. B* **2004**, *108*, 689–695. [[CrossRef](#)]
24. Yang, G.; Sun, Y.; Lv, P.; Zhen, F.; Cao, X.; Chen, X.; Wang, Z.; Yuan, Z.; Kong, X. Preparation of Pt–Ru/C as an Oxygen-Reduction Electrocatalyst in Microbial Fuel Cells for Wastewater Treatment. *Catalysts* **2016**, *6*, 150. [[CrossRef](#)]
25. Ling, Y.; Yang, Z.; Yang, J.; Zhang, Y.; Zhang, Q.; Yu, X.; Cai, W. PtRu Nanoparticles Embedded in Nitrogen Doped Carbon with Highly Stable CO Tolerance and Durability. *Nanotechnology* **2018**, *29*, 055402. [[CrossRef](#)]
26. Harish, S.; Baranton, S.; Coutanceau, C.; Joseph, J. Microwave Assisted Polyol Method for the Preparation of Pt/C, Ru/C and PtRu/C Nanoparticles and its Application in Electrooxidation of Methanol. *J. Power Sources* **2012**, *214*, 33–39. [[CrossRef](#)]
27. Chen, L.; Liang, X.; Wang, D.; Yang, Z.; He, C.-T.; Zhao, W.; Pei, J.; Xue, Y. Platinum–Ruthenium Single Atom Alloy as a Bifunctional Electrocatalyst toward Methanol and Hydrogen Oxidation Reactions. *ACS Appl. Mater. Interfaces* **2022**, *14*, 27814–27822. [[CrossRef](#)] [[PubMed](#)]
28. Takasu, Y.; Fujiwara, T.; Murakami, Y.; Sasaki, K.; Oguri, M.; Asaki, T.; Sugimoto, W. Effect of Structure of Carbon-Supported PtRu Electrocatalysts on the Electrochemical Oxidation of Methanol. *J. Electrochem. Soc.* **2000**, *147*, 4421–4427. [[CrossRef](#)]
29. Sztaberek, L.; Mabey, H.; Beatrez, W.; Lore, C.; Santulli, A.C.; Koenigsmann, C. Sol–Gel Synthesis of Ruthenium Oxide Nanowires To Enhance Methanol Oxidation in Supported Platinum Nanoparticle Catalysts. *ACS Omega* **2019**, *4*, 14226–14233. [[CrossRef](#)]
30. Rodrigues, T.S.; Zhao, M.; Yang, T.-H.; Gilroy, K.D.; da Silva, A.G.M.; Camargo, P.H.C.; Xia, Y. Synthesis of Colloidal Metal Nanocrystals: A Comprehensive Review on the Reductants. *Chem.—A Eur. J.* **2018**, *24*, 16944–16963. [[CrossRef](#)] [[PubMed](#)]
31. Tusi, M.M.; Polanco, N.S.O.; Brandalise, M.; Correa, O.V.; Silva, A.C.; Ribeiro, V.A.; Neto, A.O.; Spinacé, E.V. PtRu/Carbon Hybrid Materials Prepared by Hydrothermal Carbonization as Electrocatalysts for Methanol Electrooxidation. *Ionics* **2012**, *18*, 215–222. [[CrossRef](#)]
32. Spinace, E.V.; Vale, L.A.I.D.; Neto, A.O.; Linardi, M. Preparation of PtRu/C Anode Electrocatalysts Using NaBH<sub>4</sub> as Reducing Agent and OH<sup>-</sup> Ions as Stabilizing Agent. *ECS Trans.* **2007**, *5*, 89. [[CrossRef](#)]
33. Shimazaki, Y.; Kobayashi, Y.; Yamada, S.; Miwa, T.; Konno, M. Preparation and Characterization of Aqueous Colloids of Pt-Ru Nanoparticles. *J. Colloid Interface Sci.* **2005**, *292*, 122–126. [[CrossRef](#)] [[PubMed](#)]
34. Geng, D.; Chen, L.; Lu, G. PH Induced Size-Selected Synthesis of PtRu Nanoparticles, Their Characterization and Electrocatalytic Properties. *J. Mol. Catal. A Chem.* **2007**, *265*, 42–49. [[CrossRef](#)]
35. Quinson, J.; Neumann, S.; Wannmacher, T.; Kacenauskaite, L.; Inaba, M.; Bucher, J.; Bizzotto, F.; Simonsen, S.B.; Theil Kuhn, L.T.; Bujak, D.; et al. Colloids for Catalysts: A Concept for the Preparation of Superior Catalysts of Industrial Relevance. *Angew. Chem. Int. Ed.* **2018**, *57*, 12338–12341. [[CrossRef](#)] [[PubMed](#)]
36. Wang, Q.; Zhou, Y.-W.; Jin, Z.; Chen, C.; Li, H.; Cai, W.-B. Alternative Aqueous Phase Synthesis of a PtRu/C Electrocatalyst for Direct Methanol Fuel Cells. *Catalysts* **2021**, *11*, 925. [[CrossRef](#)]
37. Prabhuram, J.; Zhao, T.S.; Tang, Z.K.; Chen, R.; Liang, Z.X. Multiwalled Carbon Nanotube Supported PtRu for the Anode of Direct Methanol Fuel Cells. *J. Phys. Chem. B* **2006**, *110*, 5245–5252. [[CrossRef](#)]

38. Paperzh, K.O.; Alekseenko, A.A.; Volochaev, V.A.; Pankov, I.V.; Safronenko, O.A.; Guterman, V.E. Stability and Activity of Platinum Nanoparticles in the Oxygen Electroreduction Reaction: Is Size or Uniformity of Primary Importance? *Beilstein J. Nanotechnol.* **2021**, *12*, 593–606. [[CrossRef](#)]
39. Leontyev, I.N.; Belenov, S.V.; Guterman, V.E.; Haghi-Ashtiani, P.; Shaganov, A.P.; Dkhil, B. Catalytic Activity of Carbon-Supported Pt Nanoelectrocatalysts. Why Reducing the Size of Pt Nanoparticles is Not Always Beneficial. *J. Phys. Chem. C* **2011**, *115*, 5429–5434. [[CrossRef](#)]
40. Leontyev, I.N.; Guterman, V.E.; Pakhomova, E.B.; Timoshenko, P.E.; Guterman, A.V.; Zakharchenko, I.N.; Petin, G.P.; Dkhil, B. XRD and Electrochemical Investigation of Particle Size Effects in Platinum-Cobalt Cathode Electrocatalysts for Oxygen Reduction. *J. Alloy. Compd.* **2010**, *500*, 241–246. [[CrossRef](#)]
41. Nash, J.; Zheng, J.; Wang, Y.; Xu, B.; Yan, Y. Mechanistic Study of the Hydrogen Oxidation/Evolution Reaction over Bimetallic PtRu Catalysts. *J. Electrochem. Soc.* **2018**, *165*, J3378–J3383. [[CrossRef](#)]
42. Gasteiger, H.A.; Markovic, N.; Ross, P.N., Jr.; Cairns, E.J. CO Electrooxidation on Well-Characterized Platinum-Ruthenium Alloys. *J. Phys. Chem.* **1994**, *98*, 617–625. [[CrossRef](#)]
43. Arenz, M.; Mayrhofer, K.J.J.; Stamenkovic, V.; Blizanac, B.B.; Tomoyuki, T.; Ross, P.N.; Markovic, N.M. The Effect of the Particle Size on the Kinetics of CO Electrooxidation on High Surface Area Pt Catalysts. *J. Am. Chem. Soc.* **2005**, *127*, 6819–6829. [[CrossRef](#)]
44. Maillard, F.; Eikerling, M.; Cherstiouk, O.V.; Schreier, S.; Savinova, E.; Stimming, U. Size Effects on Reactivity of Pt Nanoparticles in CO Monolayer Oxidation: The role of Surface Mobility. *Faraday Discuss.* **2004**, *125*, 357–377. [[CrossRef](#)]
45. Chung, D.Y.; Lee, K.-J.; Sung, Y.-E. Methanol Electro-Oxidation on the Pt Surface: Revisiting the Cyclic Voltammetry Interpretation. *J. Phys. Chem. C* **2016**, *120*, 9028–9035. [[CrossRef](#)]
46. Petrii, O.A. The Progress in Understanding the Mechanisms of Methanol and Formic Acid Electrooxidation on Platinum Group Metals (a Review). *Russ. J. Electrochem.* **2019**, *55*, 1–33. [[CrossRef](#)]
47. Wang, Y.; Zang, J.; Dong, L.; Pan, H.; Yuan, Y.; Wang, Y. Graphitized Nanodiamond Supporting PtNi Alloy as Stable Anodic and Cathodic Electrocatalysts for Direct Methanol Fuel Cell. *Electrochim. Acta* **2013**, *113*, 583–590. [[CrossRef](#)]
48. Wang, X.; Wang, H.; Wang, R.; Wang, Q.; Lei, Z. Carbon-Supported Platinum-Decorated Nickel Nanoparticles for Enhanced Methanol Oxidation in Acid Media. *J. Solid State Electrochem.* **2012**, *16*, 1049–1054. [[CrossRef](#)]
49. Menshchikov, V.; Alekseenko, A.; Guterman, V.; Nechitailov, A.; Glebova, N.; Tomasov, A.; Spiridonova, O.; Belenov, S.; Zelenina, N.; Safronenko, O. Effective Platinum-Copper Catalysts for Methanol Oxidation and Oxygen Reduction in Proton-Exchange Membrane Fuel Cell. *Nanomaterials* **2020**, *10*, 742. [[CrossRef](#)]
50. Santasalo-Aarnio, A.; Borghei, M.; Anoshkin, I.V.; Nasibulin, A.G.; Kauppinen, E.I.; Ruiz, V.; Kallio, T. Durability of Different Carbon Nanomaterial Supports with PtRu Catalyst in a Direct Methanol Fuel Cell. *Int. J. Hydrog. Energy* **2012**, *37*, 3415–3424. [[CrossRef](#)]
51. Kabbabi, A.; Faure, R.; Durand, R.; Beden, B.; Hahn, F.; Leger, J.-M.; Lamy, C. In Situ FTIRS Study of the Electrocatalytic Oxidation of Carbon Monoxide and Methanol at Platinum–Ruthenium Bulk Alloy Electrodes. *J. Electroanal. Chem.* **1998**, *444*, 41–53. [[CrossRef](#)]
52. Guo, J.; Zhao, T.; Prabhuram, J.; Chen, R.; Wong, C. Preparation and Characterization of a PtRu/C Nanocatalysts for Direct Methanol Fuel Cell. *Electrochim. Acta* **2005**, *51*, 754–763. [[CrossRef](#)]
53. De La Fuente, J.; Perez-Alonso, F.J.; Martínez-Huerta, M.; Peña, M.A.; Fierro, J.; Rojas, S. Identification of Ru Phases in PtRu Based Electrocatalysts and Relevance in the Methanol Electrooxidation Reaction. *Catal. Today* **2009**, *143*, 69–75. [[CrossRef](#)]
54. Li, Y.; Zhu, X.; Chen, Y.; Zhang, S.; Li, J.; Liu, J. Rapid Synthesis of Highly Active Pt/C Catalysts with Various Metal Loadings from Single Batch Platinum Colloid. *J. Energy Chem.* **2020**, *47*, 138–145. [[CrossRef](#)]
55. Langford, J.I.; Wilson, A.J.C. Scherrer after Sixty Years: A Survey and Some New Results in the Determination of Crystallite Size. *J. Appl. Crystallogr.* **1978**, *11*, 102–113. [[CrossRef](#)]
56. Liu, Z.; Ling, X.Y.; Su, A.X.; Lee, J.Y. Carbon-Supported Pt and PtRu Nanoparticles as Catalysts for a Direct Methanol Fuel Cell. *J. Phys. Chem. B* **2004**, *108*, 8234–8240. [[CrossRef](#)]
57. Vega, L.; Garcia-Cardona, J.; Viñes, F.; Cabot, P.L.; Neyman, K.M. Nanostructuring Determines Poisoning: Tailoring CO Adsorption on PtCu Bimetallic Nanoparticles. *Mater. Adv.* **2022**, *3*, 4159–4169. [[CrossRef](#)]
58. Kuriganova, A.B.; Leontyeva, D.V.; Ivanov, S.; Bund, A.; Smirnova, N.V. Electrochemical Dispersion Technique for Preparation of Hybrid MO<sub>x</sub>-C Supports and Pt/MO<sub>x</sub>-C Electrocatalysts for Low-Temperature Fuel Cells. *J. Appl. Electrochem.* **2016**, *46*, 1245–1260. [[CrossRef](#)]